[5] K. F. Lee, K. M. Luk, K. F. Tong, Y. L. Yung, and T. Huynh, "Experimental and simulation studies of the coaxially-fed U-slot rectangular patch antenna," *Proc. Inst. Elect. Eng. Microwaves, Antennas and Propagation*, vol. 144, no. 5, Oct. 1997.
[6] K. F. Tong, K. M. Luk, K. F. Lee, and R. Q. Lee, "A broadband U-slot rectangular patch antenna on a microwave substrate," *IEEE Trans. Antennas Propag.*, vol. 48, no. 6, p. 954, Jun. 2000.
[7] J. R. James, P. S. Hall, and C. Wood, *Microstrip Antenna Theory and Design*. London, U.K.: Peter Peregrinus, Ltd., 1981.
[8] I. J. Bahl and P. Bhartia, *Microstrip Antennas*. New York: Artech House, 1980.

Probe Fed Stacked Patch Antenna for Wideband Applications

M. A. Matin, B. S. Sharif, and C. C. Tsimenidis

***Abstract*—A new design of a U-slot microstrip antenna with an E shaped stacked patch is presented that achieves an impedance bandwidth of 59.7%. Parameters such as substrate thickness, slot length, width are investigated and design results from parametric simulations are presented. The electric current distributions on the patch and the radiation patterns are also demonstrated in this paper.**

***Index Terms*—E-shape patch, microstrip, U-slot antenna, wideband.**

I. Introduction

Microstrip patch antennas are currently widely used particularly since they are lightweight, compact and cost effective; however, their main disadvantage is their narrow bandwidth. Therefore, various designs have been proposed in the literature to improve their bandwidth, including the use of thicker substrates, different shape patches and probes, addition of parasitic patches [1]–[4] and cutting of slots [5]–[7]. Examples of cutting slots include probe-fed U-slot patch antennas [5], double-C patch antennas [6], and E-shape patch [7] antennas which provide excellent bandwidths. The conventional U-slot patch antenna achieves an input impedance bandwidth of 30% and its impedance characteristics are further improved with electromagnetic coupling using an L-probe and stacked rectangular patch [3] which has a 44.4% bandwidth. When the two parallel slots in the U-slot patch are extended to the edge, an E-shape patch is obtained [6]–[8]. The E-shaped patch also provides wideband characteristics and the bandwidth is further increased to 44.9% by stacking a second patch above it in addition to using a washer on the probe [2]. More recent research on probe fed stacked patch for ultrawideband (UWB) applications has resulted in 54% bandwidth [4]. In this paper, we propose a wideband patch antenna with simple coaxial feed configuration based on the conventional U-slot patch antenna stacking with an E-shaped patch that is capable of achieving an impedance bandwidth of 59.7%. A SMA connector is used as a coaxial probe which is connected to the U-slot patch. The feed probe is located close to patch centre for good excitation of the proposed antenna over the wide bandwidth.

Manuscript received October 25, 2006.

The authors are with the School of Electrical, Electronic and Computer Engineering, University of Newcastle upon Tyne, Merz Court NE1 7RU, U.K. (e-mail: m.a.matin@ncl.ac.uk; bayan.sharif@ncl.ac.uk; charalampos.tsimenidis@ncl.ac.uk).

Digital Object Identifier 10.1109/TAP.2007.901924

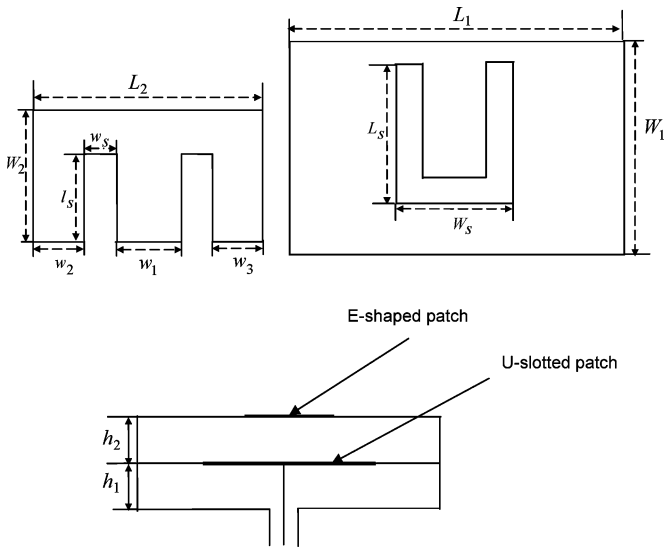

Fig. 1. Antenna structure.

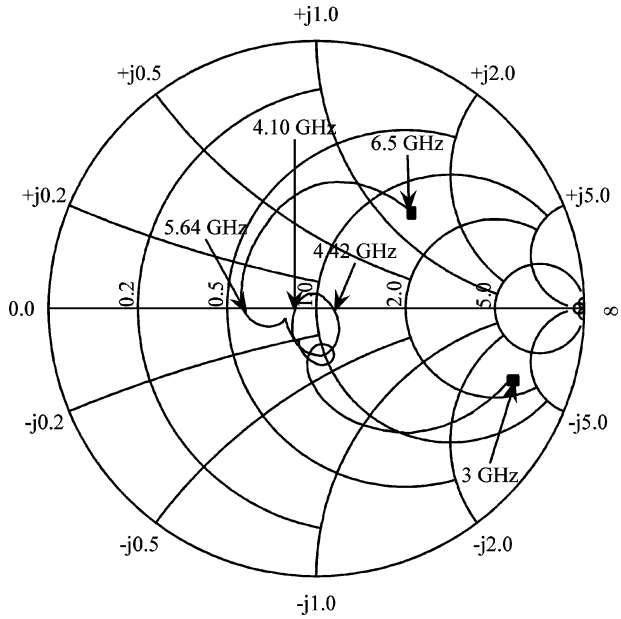

Fig. 2. The measured input impedance curves.

II. Antenna Design and Performance

The configuration of the proposed antenna is shown in Fig. 1. This antenna consists of an E-shaped upper patch and a U-slot lower patch fed by a vertical probe which is an extension of the inner conductor of a coaxial feed line. The U-slot is placed on a dielectric substrate with dielectric constant of 1.1 and thickness of 6 mm. To expand the antenna bandwidth, an E-shaped patch with another dielectric substrate is stacked on top of the lower U-slot patch. The geometrical shape of the upper patch resembles the letter "E" as two parallel slots are incorporated within it. The E-shaped patch is essentially formed by removing the lower portion of a U-slot that which has a low current distribution. Therefore, in the resulting antenna structure, more parameters can be varied than with a simple patch stacking. In this case careful optimization can be applied to control the coupling level between the patches to enhance the antenna bandwidth without splitting the operation band. A further increase in the bandwidth is also possible through incorporating a small washer to cancel the reactance of the probe at

TABLE I
PHYSICAL DIMENSIONS OF THIS STACKED ANTENNA DIMENSIONS UNIT: MILLIMETER

L_1	W_1	L_s	W_s	L_2	W_2	l_s	w_s	w_1	w_2	w_3	h_1	h_2	ε_r
39.4	**29.4**	**17**	**15.4**	**26.5**	**18**	**14.2**	**1.4**	**9.6**	**7.05**	**7.05**	**6**	**5.5**	**1.1**

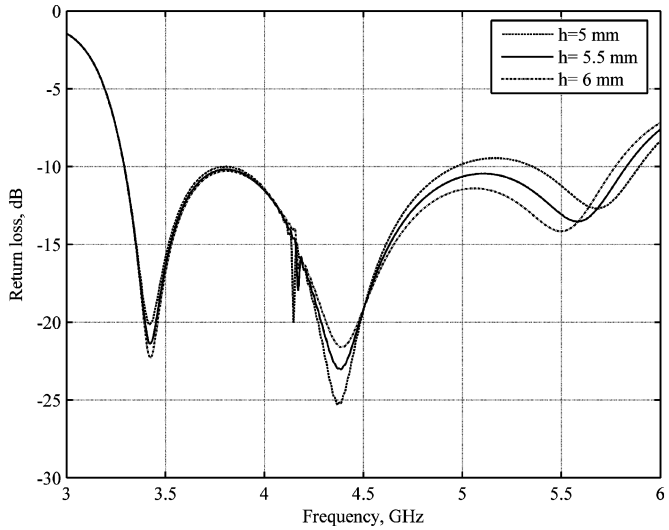

Fig. 3. simulated return loss against frequency for various distance of two patches; other parameter are the same as in Table I.

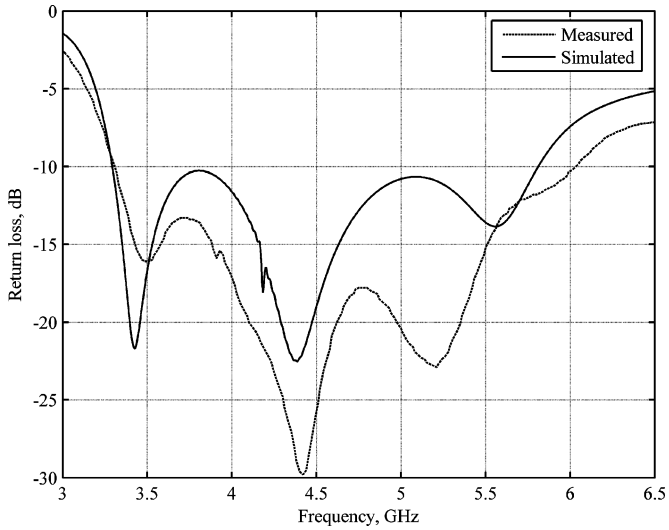

Fig. 4. The measured and simulated return loss against frequency for $h = 5.6$ mm; other parameters are the same as in Table I.

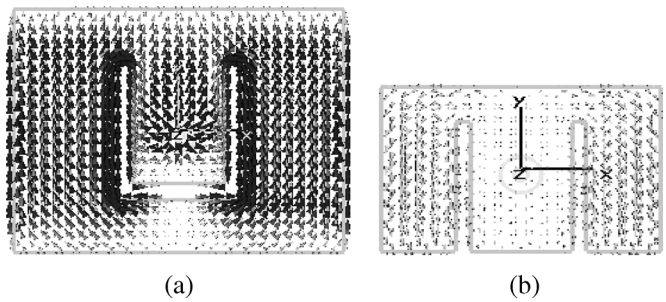

Fig. 5. The current distribution at 3.48 GHz (a) lower patch and (b) top patch.

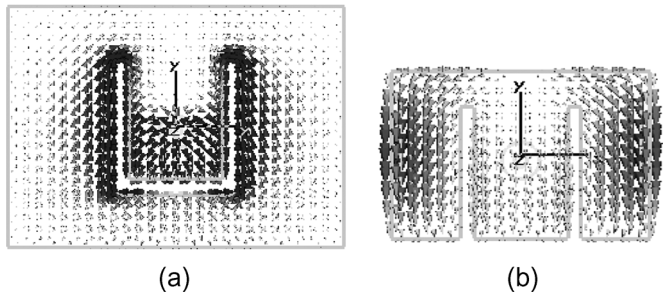

Fig. 6. The current distribution at 4.42 GHz (a) lower patch and (b) top patch.

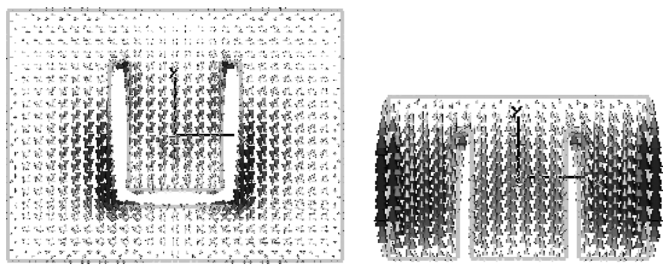

Fig. 7. The current distribution at 5.60 GHz (a) lower patch and (b) top patch.

the expense of increased complexity of the design and fabrication. The lower and upper patch dimensions are $39.4 \times 29.4\ \mathrm{mm}^2 (L_1 \times W_1)$ and $26.5 \times 18\ \mathrm{mm}^2 (L_2 \times W_2)$, respectively. Detailed dimensions of different parameters of both patches are given in Table I.

The measured input impedance of the stacked patch antenna is shown in the smith chart of Fig. 2. The resonant loops of the stacked antenna are located near the centre of the smith chart, presenting better matching input impedance. There are three resonant frequencies being generated. The small loop on the smith chart does not cross the real axis to indicate true resonant frequencies but the wideband impedance characteristic is apparent from the impedance curve. The return loss is measured using an E5071B network analyzer in an anechoic chamber.

Further numerical analyses were performed using CST Microwave Studio [9] which is a commercial software package based on the finite integral technique. The important parameters involved in the design process include the slot length, width, position and separation between patches. These parameters, which have a profound effect on the coupling between the patches, allow for the antenna's input impedance to be adjusted and good matching to be achieved. In general, the centre wing and the two side wings of E-shaped patch form two resonance frequencies as the interaction of the slot with its own patch forms two resonance frequencies. Therefore stacking with an E-shape patch will, at least, provide four resonance frequencies and prudent selection of these frequencies can enhance the impedance bandwidth. It is observed that the present structure with good matching could be implemented when two patches are centred along a common axis.

Fig. 4 shows the simulated and measured return loss curves. The 10 dB return loss is from 3.275–6.07 GHz (measured) and

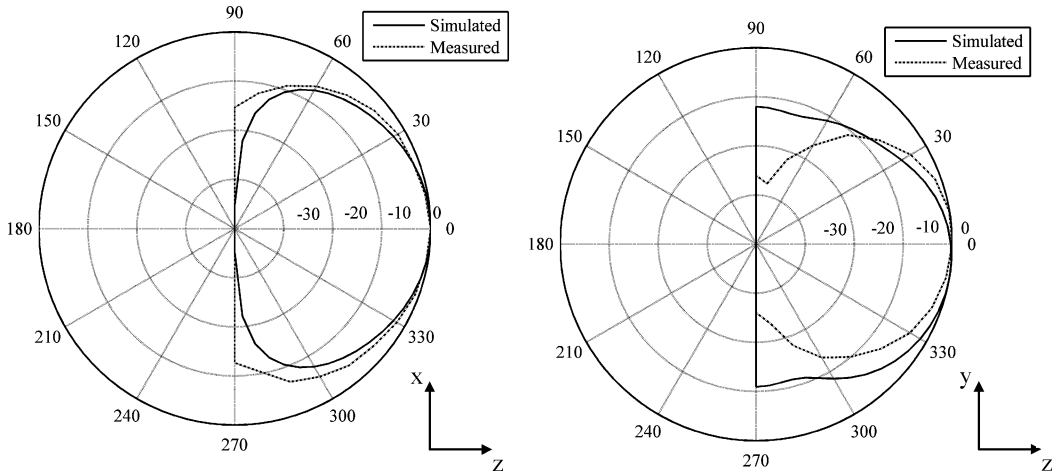

Fig. 8. Simulated (solid line) and measured (dotted line) radiation pattern at 3.49 GHz (a) XZ-plane and (b) YZ-plane.

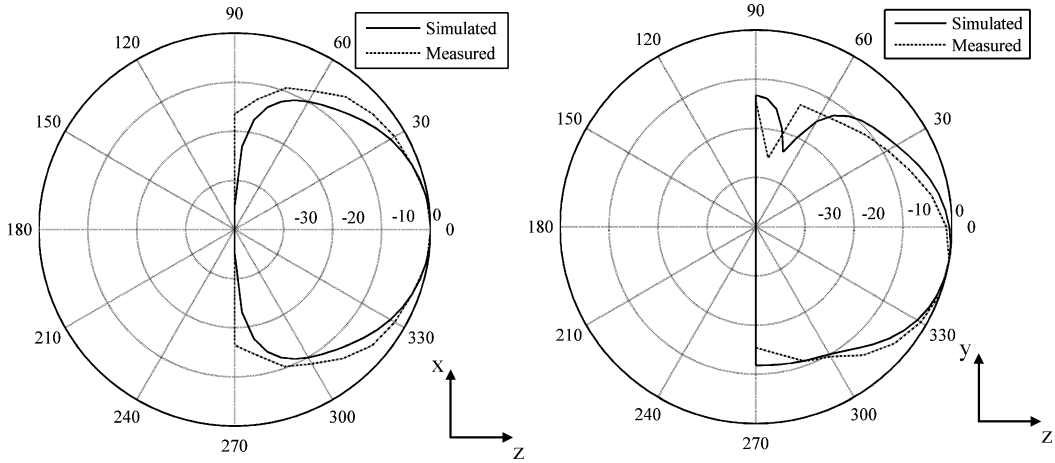

Fig. 9. Simulated (solid line) and measured (dotted line) radiation pattern at 4.42 GHz (a) XZ-plane and (b) YZ-plane.

3.27–5.85 GHz (simulated). The obtained measurement confirms the wideband characteristic of the proposed design predicted by the simulation, albeit with a slight discrepancy which is probably due to imperfection in the fabrication process.

III. Antenna Characteristics

Various parameters are investigated such as the distance between two patches and the slot length and width of the E-shaped patch. It is found that a good impedance matching can be obtained through coupling between the patches up to a certain value. However, with further increase in coupling, the impedance matching deteriorates, showing that over coupling can also degrade the impedance matching as can under coupling. When, $h_2 = 5.5$ mm the maximum bandwidth is achieved in the frequency range 3.28–5.85 GHz which is shown in Fig. 3. However, as h_2 increases the return loss decreases at 4.38 GHz and hence degrades impedance matching. The distance between patches mainly affects the frequency corresponding to the upper edge of the bandwidth, whereas it has minimal effect on the frequency corresponding to the lower edge. It is also found that the higher frequency with -10 dB return loss is not affected by the variation of the slot width and length of the E-shaped patch. However, the lower frequency with -10 dB loss slightly changes with an increase in the slot width and length. Detailed studies of the various parameters are not included in this paper.

The simulated current distributions at different frequencies are presented in Figs. 5, 6, and 7. In Fig. 5, it is observed that the surface currents at the lower patch originate behind the U-slot, and are strong on the patch outside the slot. Due to the presence of the U-slot, the surface currents at $f_1 = 3.48$ GHz are forced to travel around it. The situation is different at $f_2 = 4.42$ GHz, where the surface current at the lower patch has a strong component at the patch centre and the area around the slot, in addition to the excitation of the two side wings of E-shaped parasitic patch. It is seen in Fig. 6 that the centre wing of the E-shaped patch is also well excited at $f_3 = 5.60$ GHz.

The radiation patterns have been simulated and also measured in an anechoic chamber at different frequencies which is illustrated in Figs. 8, 9, and 10. Furthermore, the experimental results are observed be in agreement with the simulated results. In the $x-z$ plane, the 3 dB beam width is 66.3 degree at 3.49 GHz, 57.8 degrees at 4.42 GHz and 64 degree at 5.2 GHz and the radiation patterns are almost similar. In the $y-z$ plane, the 3 dB beamwidth is 58.4 degrees at 3.49 GHz, 48.3 degrees at 4.42 GHz and 50.2 degrees at 5.2 GHz. A tilt of the $y-z$ plane main lobe direction around the z-axis direction is observed with a maximum beam squint of 15°. The average gain of the antenna is about, 8 dBi $\pm$ 1.4 dBi across the matching band. The radiation efficiency which is used to relate the gain and directivity is not significantly affected by dielectric losses. Furthermore, due to thicker substrate, the fabricated antenna reduces conductor loss and is also mechanically strong. The ground plane effect is also a critical factor; however, its dimension is sufficient for proper operation of the antenna.

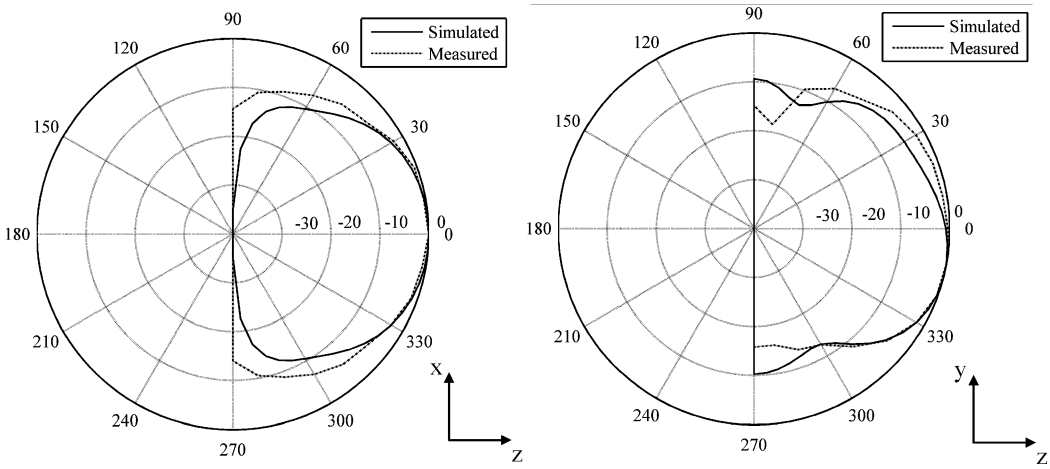

Fig. 10. Simulated (Solid line) and measured (dotted line) radiation pattern at 5.2 GHz (a) XZ-plane and (b) YZ-plane.

IV. Conclusion

A low cost, compact U-slotted patch stacking with E-Shape patch has been presented in this paper which was simulated, fabricated, measured and analyzed. The return loss of the proposed structure is -10 dB across the band frequency 3.28–6.07 GHz which shows 5.7% increase in bandwidth in comparison to the patch antenna with two E-shaped stacked patches. The radiation patterns are relatively constant throughout the whole bandwidth.

References

[1] K. Q. Lee, K. F. Lee, and J. Bobnchak, "Characteristics of a two layer electromagnetically coupled rectangular patch antenna," *Electron. Lett.*, vol. 23, pp. 1070–1072, 1987.

[2] B.-L. Ooi, S. Qin, and M.-S. Leong, "Novel design of broadband stacked patch antenna," *IEEE Trans. Antennas Propag.*, vol. 50, no. 10, pp. 1391–1395, Oct. 2002.

[3] B. L. Ooi and C. L. Lee, "Broadband air-filled stacked U-slot patch antenna," *Electron. Lett.*, vol. 35, no. 7, pp. 515–517, Apr. 1, 1999.

[4] H. Ghannoum, S. Bories, and C. Roblin, "Probe fed stacked patch antenna for UWB sectoral applications," in *Proc. IEEE International Conf. on Ultra-Wideband (ICU)*, Sep. 2005, pp. 97–102.

[5] K. F. Lee, K. M. Luk, K. F. Tong, S. M. Shum, T. Huynk, and R. Q. Lee, "Experimental and simulation studies of the coaxially fed u-slot rectangular patch antenna," *Proc. Inst. Elect. Eng. Microw. Antenna Propag.*, vol. 144, no. 5, pp. 354–358, Oct. 1997.

[6] M. Sanad, "Double C-patch antennas having different aperture shapes," in *Proc. IEEE AP-S Symp.*, Newport Beach, CA, Jun. 1995, pp. 2116–2119.

[7] F. Yang, X. X. Zhang, X. Ye, and Y. Rahmat-Samii, "Wide-band E-shaped patch antennas for wireless communications," *IEEE Trans. Antennas Propag.*, vol. 49, no. 7, pp. 1094–1100, Jul. 2001.

[8] K. L. Wong and W. H. Hsu, "A broadband rectangular patch antenna with a pair of wide slits," *IEEE Trans. Antennas Propag.*, vol. 49, no. 9, pp. 1345–1347, Sep. 2001.

[9] *"CST Microwave Studio, User Manual Version 2006,"* CST GmbH, Sep. 2005.

A Resonant Extraction Method for Installed Antenna Radiation Calculations

Morui Li and Cai-Cheng Lu

***Abstract*—In the calculation of the radiation patterns of antennas installed on complex structures using iterative solvers, the convergence rate is often slower compared to the problem with the structure alone without antenna. This is due to the resonant nature of the antenna. To increase the convergence rate, a resonant extraction method is introduced by which a small region including the antenna and its nearby neighborhood is singled out from the overall structure and treated using a direct method, and a reduced system is better conditioned, hence much less iteration numbers are needed if solved by an iterative solver. Numerical examples are provided to demonstrate the effectiveness of this method.**

***Index Terms*—Antenna simulation, integral equation, iterative solver, precondition method.**

I. Introduction

In many realistic applications, antennas, such as the microstrip patch and monopoles, are often mounted on large complex structures such as satellites, aircrafts, and vehicles. Under such situations, the antenna pattern may be substantially deformed due to the interference of the platform. The interference must be taken into account in installed antenna simulation to achieve accurate results. A number of approaches have been proposed [1]–[4] to solve such problems, including the integral equation approach. The integral equation formulation uses the unbounded space Green's function, hence, it automatically includes the interactions between the antenna and the platform. More importantly, the application of fast solvers such as the multilevel fast multipole algorithm (MLFMA) [5] made it possible for the integral equation approach to solve problems with electrically-large-sized platforms. The fast solver significantly reduced the computational complexity for the integral equation approach. In this case, the low rate of convergence for some problems becomes a bottleneck in efficiency. Efforts have been

Manuscript received June 19, 2006; revised March 28, 2007.

The authors are with the University of Kentucky, Lexington, KY 40506 USA (e-mail: cclu@engr.uky.edu).

Color versions of one or more of the figures in this paper are available online at http://ieeexplore.ieee.org.

Digital Object Identifier 10.1109/TAP.2007.901872